

10552

NACA TN 4213

# NATIONAL ADVISORY COMMITTEE FOR AERONAUTICS

0066838



TECH LIBRARY KAFB, NM

TECHNICAL NOTE 4213

RECOVERY TEMPERATURES AND HEAT TRANSFER NEAR  
TWO-DIMENSIONAL ROUGHNESS ELEMENTS AT MACH 3.1

By Paul F. Brinich

Lewis Flight Propulsion Laboratory  
Cleveland, Ohio



Washington  
February 1958

TECHNICAL LIBRARY  
AFL 2811



0066838

## NATIONAL ADVISORY COMMITTEE FOR AERONAUTICS

## TECHNICAL NOTE 4213

RECOVERY TEMPERATURES AND HEAT TRANSFER NEAR TWO-DIMENSIONAL  
ROUGHNESS ELEMENTS AT MACH 3.1

By Paul F. Brinich

## SUMMARY

An investigation was made to determine the effect of single and multiple two-dimensional roughness elements on the temperature distribution, the pressure distribution, and the heat transfer at Mach 3.1. A hollow cylinder and a cone-cylinder model were used.

Abrupt perturbations in surface temperature occurred in the neighborhood of the elements when the boundary layer was turbulent, but were absent when it was laminar. The type of perturbation depended on the element shape, forward-facing wedges giving the lowest temperatures immediately behind the element and forward-facing steps the highest. For a turbulent boundary layer the heat-transfer rate behind the wedge element was less than that obtained immediately ahead of the element.

## INTRODUCTION

This report is an extension of the investigation of reference 1, in which the equilibrium surface temperature of an insulated body having laminar, transitional, and turbulent flow was studied. The previous investigation considered the effects of single circular wire roughness elements on the surface temperature distribution on a hollow insulated cylinder having its axis aligned with the airflow at Mach 3.1. Reference 1 found that the surface temperature distribution in the neighborhood of a roughness element had certain characteristics which depended on whether the boundary layer over the element was laminar, transitional, or turbulent. When the flow was laminar, no effect on the surface temperature near the element could be found; but, when the flow was turbulent, abrupt perturbations in the surface temperature were observed, the effect of which extended appreciable distances downstream of the elements.

After these observations were made it was natural to speculate as to the possibility of controlling the recovery temperature over extended portions of the model when the flow was turbulent by properly shaping the

4196

CW-1

roughness element or by using multiple elements. In addition, the heat transferred to the body could perhaps be reduced by the use of such roughness elements.

The present investigation was undertaken to give preliminary answers to these questions. The hollow-cylinder model could not be used to obtain heat-transfer data; therefore, for this phase of the test program a smaller-diameter cone-cylinder model was used. All tests were conducted in the Lewis 1- by 1-foot variable Reynolds number wind tunnel at Mach 3.1, which is the same test facility used in reference 1.

4796

## SYMBOLS

$C_p$	pressure coefficient, $(p - p_\infty)/q_\infty$
$c_{p,a}$	specific heat at constant pressure for air
$c_{p,b}$	specific heat at constant pressure for monel model
$h$	heat-transfer coefficient (dimensional)
$k_b$	thermal conductivity of monel model
$p$	static pressure
$p_\infty$	static pressure of free stream
$q$	heat-transfer rate
$q_\infty$	free-stream dynamic pressure
St	Stanton number, dimensionless heat-transfer coefficient = $\frac{h}{\rho_\infty u_\infty c_{p,a}} = \frac{h}{(\rho u c_{p,a})_\infty}$
$T_{aw}$	adiabatic wall temperature
$T_t$	stagnation temperature
$T_w$	wall surface temperature
$T_\infty$	free-stream temperature
$t$	time, sec
$u_\infty$	free-stream velocity ahead of model

x	distance from tip
$\eta$	temperature-recovery factor, $(T_w - T_\infty) / (T_t - T_\infty)$
$v_\infty$	free-stream kinematic viscosity
$\rho_b$	density of monel model
$\rho_\infty$	free-stream air density ahead of model
$\tau$	thickness of model skin

4196

GW-1 back

## APPARATUS AND PROCEDURE

## Models and Roughness Elements

The hollow-cylinder model used in the present investigation (fig. 1(a)) had a 5.31-inch outside diameter and was 27.4 inches long. The thickness of the leading edge was about 0.001 inch, which is sufficiently sharp to have negligible bluntness effects on the location of transition and on the boundary-layer development. The outer skin was of 0.032-inch stainless steel and was thermally insulated from the flow through the interior of the cylinder. The same model was used in the tests reported in reference 1.

The  $9\frac{1}{2}^\circ$ -included-angle cone-cylinder model of 1.75-inch outside diameter and 18-inch length that was used for the heat-transfer measurements is shown in figure 1(b). The wall of the cone-cylinder model was constructed of "K" monel of 0.062-inch nominal thickness. Heat transfer between the model and the stream was obtained by first enclosing the model within shoes into which liquid nitrogen was pumped. After the model was cooled by the liquid nitrogen to a temperature of  $-343^\circ F$ , the shoes were sprung apart and retracted, exposing the model to the relatively warm ( $T_t = 80^\circ F$ ) tunnel airstream. The construction of the cone-cylinder model and the precooling apparatus are described in detail in reference 2. Both models were tested in a stream having a Mach number of 3.1 and a unit Reynolds number range of  $1 \times 10^5$  to  $7 \times 10^5$  per inch.

For the present tests, wire elements 0.080 inch high having circular, wedge, and diamond cross sections, and one 0.160-inch-high wedge were used. These elements, shown in figure 2, include those for both the hollow-cylinder and the cone-cylinder models. Most of these elements were made of carbon steel. Surface finishes on the elements as well as on the models were approximately of 8-microinch (average) irregularity. The 0.080-inch elements correspond to the largest roughness elements tested in reference 1.

### Reduction of Data

Equilibrium surface temperatures on the hollow cylinder were obtained from the electrical output of the stainless-steel - constantan thermocouples in the model surface. Outputs were measured on a self-balancing recording potentiometer, which gave accuracies of  $\pm 0.5^\circ$  F. Recovery factors on the hollow cylinder were computed from the following equation:

$$\eta = \frac{T_w - T_\infty}{T_t - T_\infty} \quad (1)$$

where  $T_w$ ,  $T_\infty$ , and  $T_t$  are the surface, free-stream, and total temperatures, respectively. Errors in recovery factor were less than 0.002. A free-stream Mach number of 3.1 was used in the calculations.

Heat-transfer measurements in the vicinity of the single wedge element were made from temperature-time records obtained from a multichannel recording oscilloscope. The surface temperatures computed from these records were accurate to  $\pm 3^\circ$  F at the low temperatures and  $\pm 1^\circ$  F near equilibrium. The equation governing the heat balance at any point on the cylindrical part of the model is given by

$$\begin{aligned} q_{\text{total}} &= c_{p,b} \rho_b \tau \frac{\partial T_w}{\partial t} \\ &= q_{\text{convected}} + q_{\text{conducted}} \\ &= h(T_{aw} - T_w) + k_b \tau \frac{\partial^2 T_w}{\partial x^2} \end{aligned} \quad (2)$$

Measured values of the adiabatic wall temperature  $T_{aw}$  were used when the flow was turbulent, theoretical values when the flow was laminar.

The heat-transfer results presented herein are in terms of the Stanton number, which is defined by the equation

$$St = \frac{h}{\rho_\infty u_\infty c_{p,a}} = \frac{q_{\text{total}} - q_{\text{conducted}}}{\rho_\infty u_\infty c_{p,a} (T_{aw} - T_w)} \quad (3)$$

The error in the Stanton number calculation is analyzed in reference 3; this analysis is valid for the present instance except for the effect of conduction. Reference 3 states that the maximum possible error in Stanton number is  $\pm 16$  percent when longitudinal conduction is negligible. In the present investigation large gradients in surface temperature are present

that cause a considerable quantity of heat to be conducted in the model skin and hence make it necessary to include an estimate of the conducted heat in equation (3). Since a calculation of the conducted heat involves evaluation of the second derivative of the temperature distribution, it is difficult to obtain an accurate estimate. The error in conducted heat, based on various possible fairings of the temperature distribution, can be as high as 100 percent. In the worst case (when the flow is laminar ahead of the element) the conducted heat can be as much as one-third of the net heat flow. When the flow is turbulent ahead of the element, however, the heat flow by conduction in the skin is a much smaller part of the net heat flow, and a much smaller error in the Stanton number should result. Since the flow downstream of the element is always turbulent, errors in conducted heat transfer there should generally be small.

## RESULTS AND DISCUSSION

### Recovery Temperatures

Recovery-temperature distribution for smooth model. - Distributions of temperature recovery factor are presented in figure 3 for the smooth hollow-cylinder model at four values of unit Reynolds number. Peak temperatures at  $x = 3.7, 5.4, 7.4$ , and 12 inches indicate points of transition from laminar to turbulent flow as defined in reference 1. These recovery-factor distributions are to be used as references with which the distributions obtained with various elements can be compared. Points to the left of the temperature peaks are in a predominantly laminar region, whereas those to the right are in turbulent flow. The region in the vicinity of the peaks is considered transitional.

Effect of element shape. - Recovery-factor distributions obtained with the several basic element shapes shown in figure 2 are plotted in figure 4 at unit Reynolds numbers of 6.8, 3.5, 1.9, and  $1.0 \times 10^5$  per inch. These unit Reynolds numbers correspond closely to the test conditions used in obtaining the results shown in figure 3. Parts of the recovery-factor distributions of figure 3 are indicated for reference purposes by a heavy solid line. Elements were located at or near  $x = 12$  inches, the exact position being indicated in the key of figure 4.

A study of figures 4(a) to (c), in which the element was placed in a turbulent boundary layer, shows that the temperature rise ahead of and over the element can be increased by use of a forward-facing step and can be kept near the normal turbulent level by use of a forward-facing wedge. The cylindrical wire element usually has an intermediate effect between these two extremes.

The temperature variations downstream of the element can be divided into two regions. The first occurred immediately downstream of the

element, where the largest temperature reduction (lowest recovery factor) was reached with a forward-facing wedge and the least with a forward-facing step. The second region occurred downstream of  $x = 15$  inches, where the over-all temperature level was depressed below the undisturbed (no element) turbulent value regardless of element shape. The length of this second region cannot be ascertained from the results shown in figure 4. As shown in figures 3(a) and (d) of reference 1, this region extends to about 12 inches downstream of the cylindrical elements. Another feature of figures 4(a) to (c) is that the largest recovery temperature reductions were reached at the highest unit Reynolds number and with the largest forward-facing wedge. This fact seems to indicate that the ratio of element height to boundary-layer thickness is significant, as was also demonstrated with cylindrical wire elements in reference 1.

The recovery factors shown in figure 4(d) were obtained when the element was placed at the natural transition point,  $x = 12$  inches. At this position the presence of the element did not affect the location of transition but increased the peak recovery factor. All element shapes increased the surface temperature immediately ahead of the element, and at a sufficient distance downstream reduced it below the smooth surface temperature level. Although it is not apparent from the figures, it should be recalled from reference 1 that when laminar flow existed over the element no perturbation in surface temperature in the neighborhood of the element occurred. (In this case the primary effect was the reduction of transition distance.)

The recovery-factor distribution in the neighborhood of the elements may be thought to have a doubtful significance because of the large temperature gradients and presumably large attendant heat-transfer rates. However, this does not present any serious problems, as shown by unpublished tests run on low-conductivity Fiberglas cylinder shells. For equivalent element sizes and shapes the recovery factors measured on the low-conductivity model differed only slightly from those reported herein.

Simultaneous pressure and temperature measurements in the neighborhood of an element. - With respect to surface temperature reduction the forward-facing wedge was the most effective of the various shapes tested. The static-pressure distributions near the element were also measured for this element. These results are presented in figure 5 for four values of the unit Reynolds number with the 0.08-inch-high wedge element 12 inches from the leading edge.

When the flow was turbulent (figs. 5(a) to (c)) there was an abrupt pressure rise at the forward edge of the element, in contrast to the transitional case (fig. 5(d)) where there was an effect of pressure feedback to a distance of 1/2 inch ahead of the element. This feedback is caused by separation ahead of the wedge. Also, the pressures returned to normal more quickly when the flow was turbulent than when it was transitional. The lowest pressure coefficient was reached for the largest unit

Reynolds number when the ratio of boundary-layer thickness to element height was small. These pressure trends with Reynolds number have also been observed in a base-pressure investigation (ref. 4).

One of the most outstanding characteristics indicated by figure 5 is the rapidity with which the pressure perturbation becomes smooth compared with the temperature perturbation. A possible cause for the more extended temperature perturbation would appear to be conduction in the model skin, as suggested in reference 1. This suggestion is contradicted by the more recent temperature measurements made on a low-conductivity Fiberglas model (discussed earlier), which showed that the skin conductivity had a small effect on the temperature distribution. The long distances downstream of the element for which depressed temperatures exist are probably caused by a distortion of the turbulent-boundary-layer profile in passing over the element.

Effect of element spacing. - The effect of spacing two 0.080-inch wedge elements in tandem with the purpose of extending the surface temperature reduction over a greater length is shown in figure 6. For this particular test a large temperature drop behind each element was realized if the spacing from one element to the next was at least 2 inches. At spacings greater than 2 inches the elements tended to act independently. For smaller element spacings the flow over the elements tended to bridge the gap between them, resulting in a smaller temperature drop after the first element. Although these characteristics are quoted for tests conducted at a unit Reynolds number of about  $6.5 \times 10^5$  per inch, substantially the same trends were observed at lower unit Reynolds numbers when the flow was turbulent, which indicates that the effect of element spacing is almost independent of boundary-layer thickness for the range of conditions investigated.

Figure 7 shows the effect of a series of 0.160-inch-high elements spaced 2 inches apart, all in the turbulent-boundary-layer region. For this case the recovery temperature was depressed to an average value very near the laminar value over the region where the elements were placed. It thus appears that the temperature reduction can be repeated a great number of times without reducing the effectiveness of the elements in depressing the temperature level. It should be mentioned that the data points appearing directly above the elements in figure 7 were obtained by thermocouples on the walls rather than on the elements. An important question that remains to be answered is whether the heat transfer as well as the surface temperature is reduced.

#### Heat Transfer

Heat-transfer measurements were made in the vicinity of a single 0.080-inch-high wedge element located on the cone-cylinder model as shown

in figure 1(b). Convective heat-transfer rates were computed by correcting the total heat flow for conduction from equation (2) and the temperature distributions shown in figure 8. The convective heat transfers were converted to Stanton numbers by use of equation (3) and are presented in figure 9.

Figure 9(a) presents the Stanton number as a function of the Reynolds number  $u_\infty x/v_\infty$  when the flow ahead of the element was laminar, and figure 9(b) when the flow ahead of the element was turbulent. Laminar flows existed when the surface temperature on the cone cylinder was low enough to stabilize the boundary layer and preserve laminar flows up to the element. Such was the case for almost the first 30 seconds of the test. Thereafter, as shown by figure 9(b), the flow ahead of the element was turbulent. Downstream of the element the flow was always turbulent.

Figure 9(a) shows that during the first 25 seconds the experimental Stanton numbers were about midway between the theoretical laminar cone and cylinder values ahead of the element. Behind the element the heat transfer increased to the theoretical turbulent flat-plate value. The turbulent theoretical value shown is for a wall to stream temperature ratio of 1.6, which is an average value for the time interval of 30 seconds considered in figure 9(a).

Figure 9(b) shows the Stanton number when the flow ahead of the element was turbulent. The heat transfer in this case was about 15 percent lower behind the element than it was ahead of the element. Theoretical turbulent Stanton numbers for an average wall to free-stream temperature ratio of 2.6 are also indicated. The results of figure 9 therefore show that, early in time when the flow ahead of the element is laminar, the element promotes turbulent flow with attendant high convective heat-transfer rates. When the flow is turbulent ahead of the element, however, the heat transfer behind the element is reduced slightly below the turbulent value.

In the preceding calculations the presence of the solid wedge element was not considered, either in the calculation of the total heat transfer or the conducted heat transfer. It would be expected that the presence of the element might tend to reduce the heat transfer behind the element. The magnitude of this heat-transfer reduction would be difficult to compute in view of the uncertain thermal connection between the element and the model skin. In all likelihood the reduction would be small, particularly at the most downstream station, since the element mass is relatively small compared with that of the model wall.

#### SUMMARY OF RESULTS

The following results were obtained from a wind-tunnel study of the effect of roughness elements on recovery temperatures and heat transfer on a hollow cylinder and a cone-cylinder:

4196  
4W-2

1. Abrupt perturbations in surface temperature occurred in the neighborhood of the elements when the boundary layer was turbulent but were absent when the boundary layer was laminar. The type of perturbation depended on the element shape; forward-facing wedges gave the lowest temperature immediately behind the element, and forward-facing steps the highest.

2. The presence of a single element caused a very abrupt perturbation in pressure that was completely smoothed out within 5 or 10 element heights when the boundary layer was turbulent.

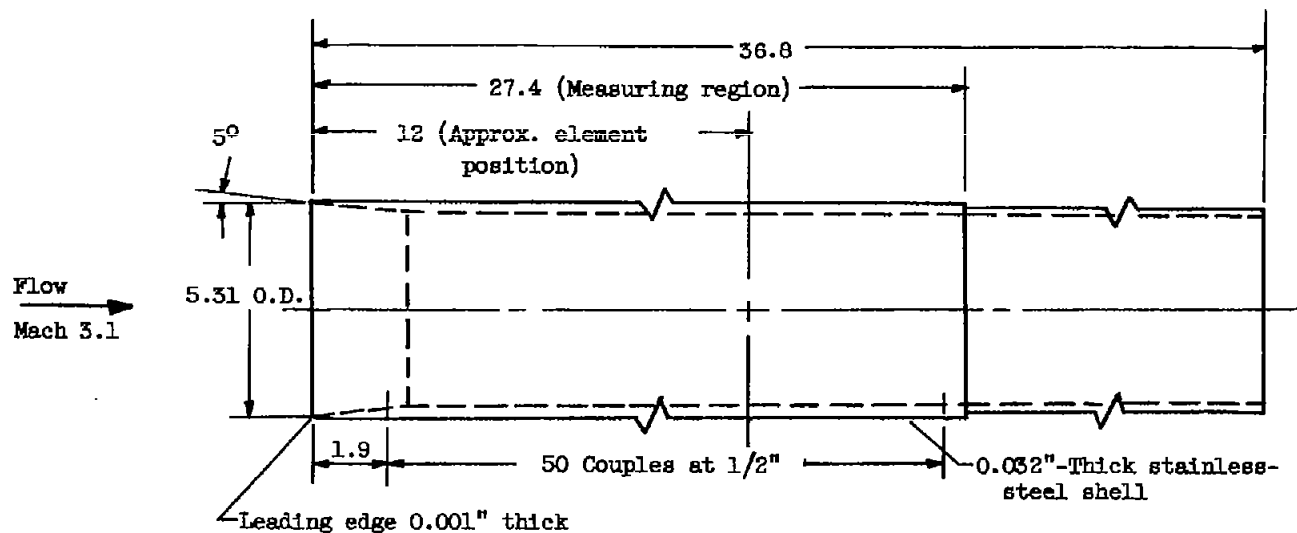
3. Multiple wedge elements retained their full effectiveness in reducing the temperature at wedge spacings greater than 2 inches. No limitation was found to the number of wedges that could be placed in tandem and yet retain effectiveness in depressing the surface temperature. The maximum number of wedges tested in tandem was five.

4. When the flow at the wedge was turbulent, the heat-transfer rate behind the wedge was diminished compared with that just upstream.

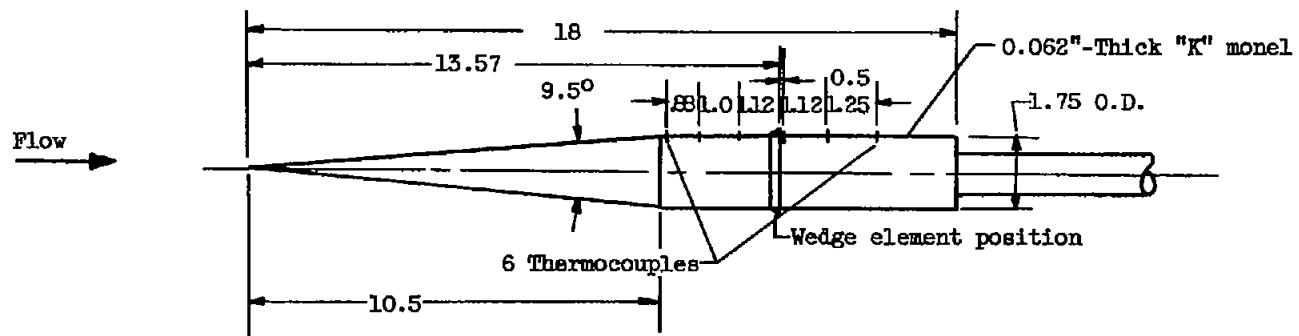
Lewis Flight Propulsion Laboratory  
National Advisory Committee for Aeronautics  
Cleveland, Ohio, November 19, 1957

#### REFERENCES

1. Brinich, Paul F.: A Study of Boundary-Layer Transition and Surface Temperature Distributions at Mach 3.12. NACA TN 3509, 1955.
2. Jack, John R., and Diaconis, N. S.: Variation of Boundary-Layer Transition with Heat Transfer on Two Bodies of Revolution at Mach Number of 3.12. NACA TN 3562, 1955.
3. Jack, John R., and Diaconis, N. S.: Heat-Transfer Measurements on Two Bodies of Revolution at a Mach Number of 3.12. NACA TN 3776, 1956.
4. Jack, John R., and Burgess, Warren C.: Aerodynamics of Slender Bodies at Mach Number of 3.12 and Reynolds Numbers from  $2 \times 10^6$  to  $15 \times 10^6$ . I - Body of Revolution with Near-Parabolic Forebody and Cylindrical Afterbody. NACA RM E51HL3, 1951.
5. Chapman, Dean R., and Rubesin, Morris W.: Temperature and Velocity Profiles in the Compressible Laminar Boundary Layer with Arbitrary Distribution of Surface Temperature. Jour. Aero. Sci., vol. 16, no. 9, Sept. 1949, pp. 547-565.
6. Lee, Dorothy, and Faget, Maxime A.: Charts Adapted from Van Driest's Turbulent Flat-Plate Theory for Determining Values of Turbulent Aerodynamic Friction and Heat-Transfer Coefficients. NACA TN 3811, 1956.



(a) Hollow-cylinder model.

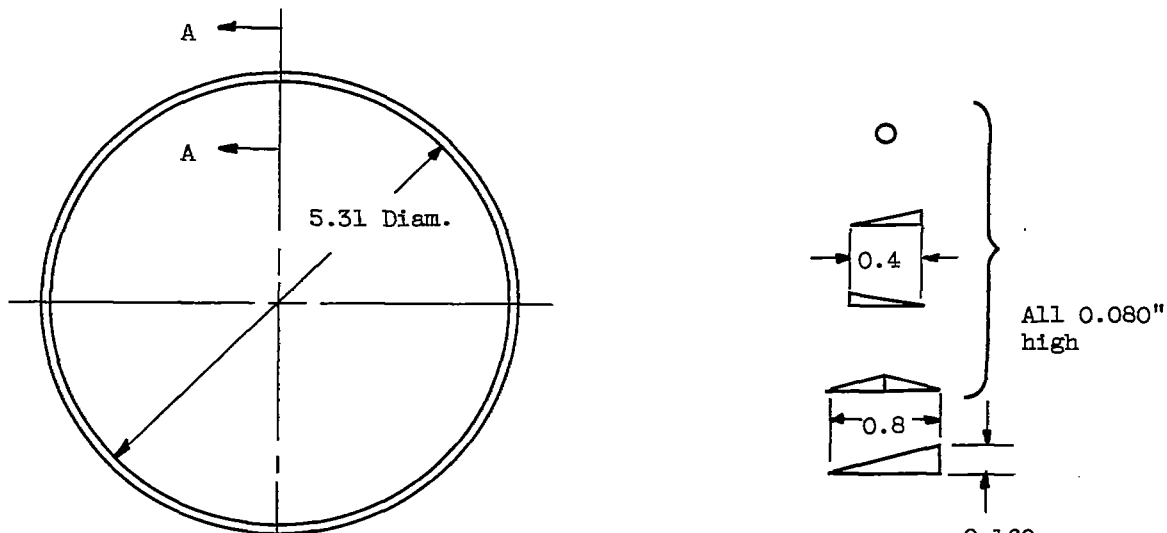


(b) Cone-cylinder heat-transfer model.

Figure 1. - Models investigated (dimensions in inches).

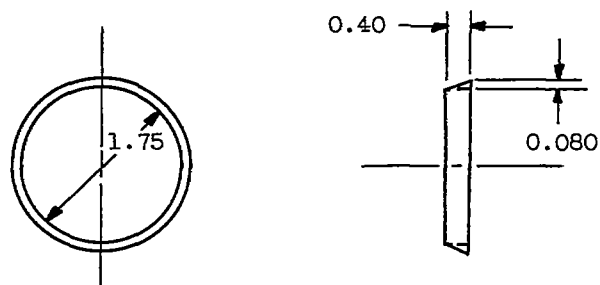
4196

CW-2 back



Sections A-A

(a) Elements for hollow-cylinder model.



(b) Element for cone-cylinder model.

Figure 2. - Roughness-element shapes used (dimensions in inches).

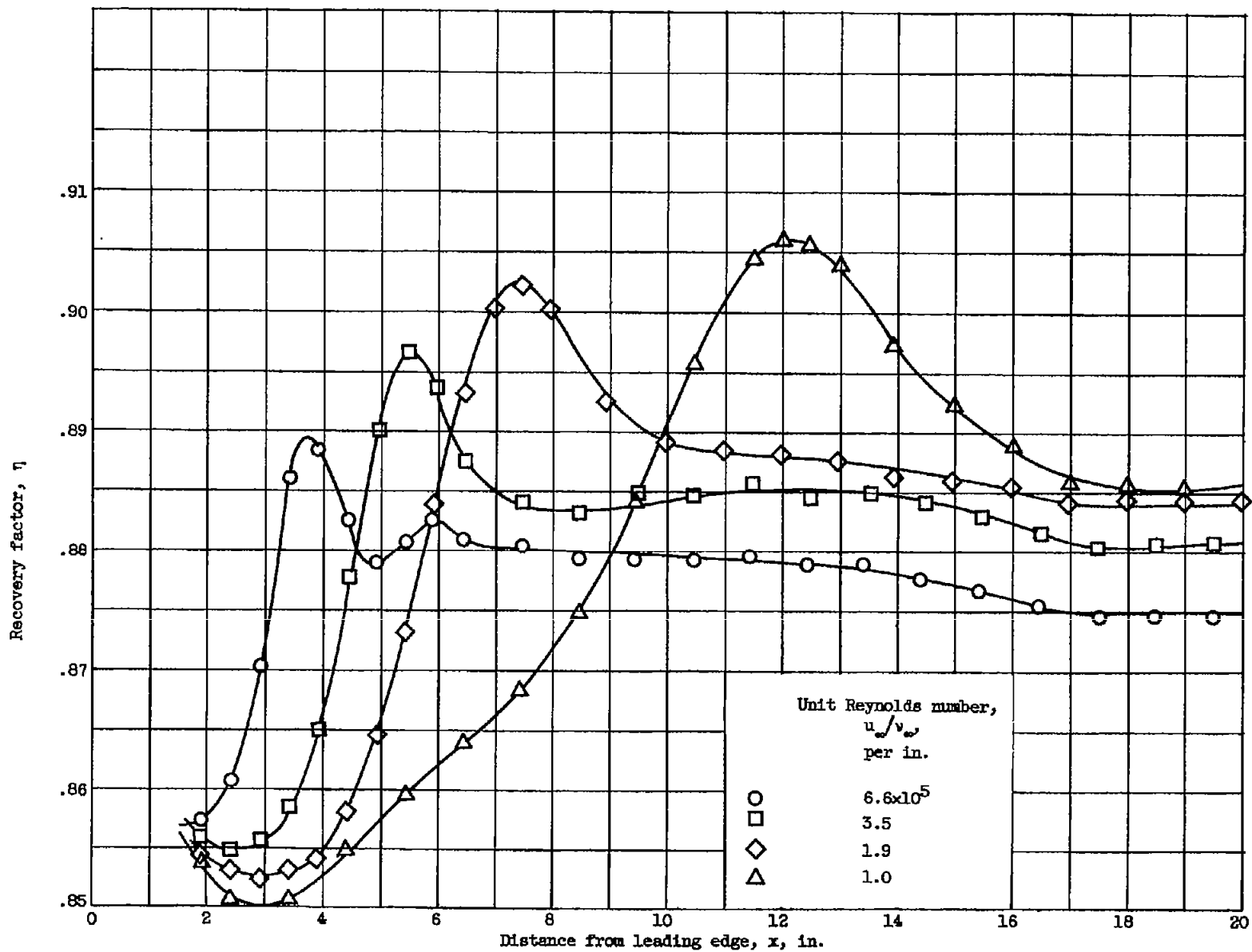


Figure 3. - Recovery-factor distributions without surface roughness elements.

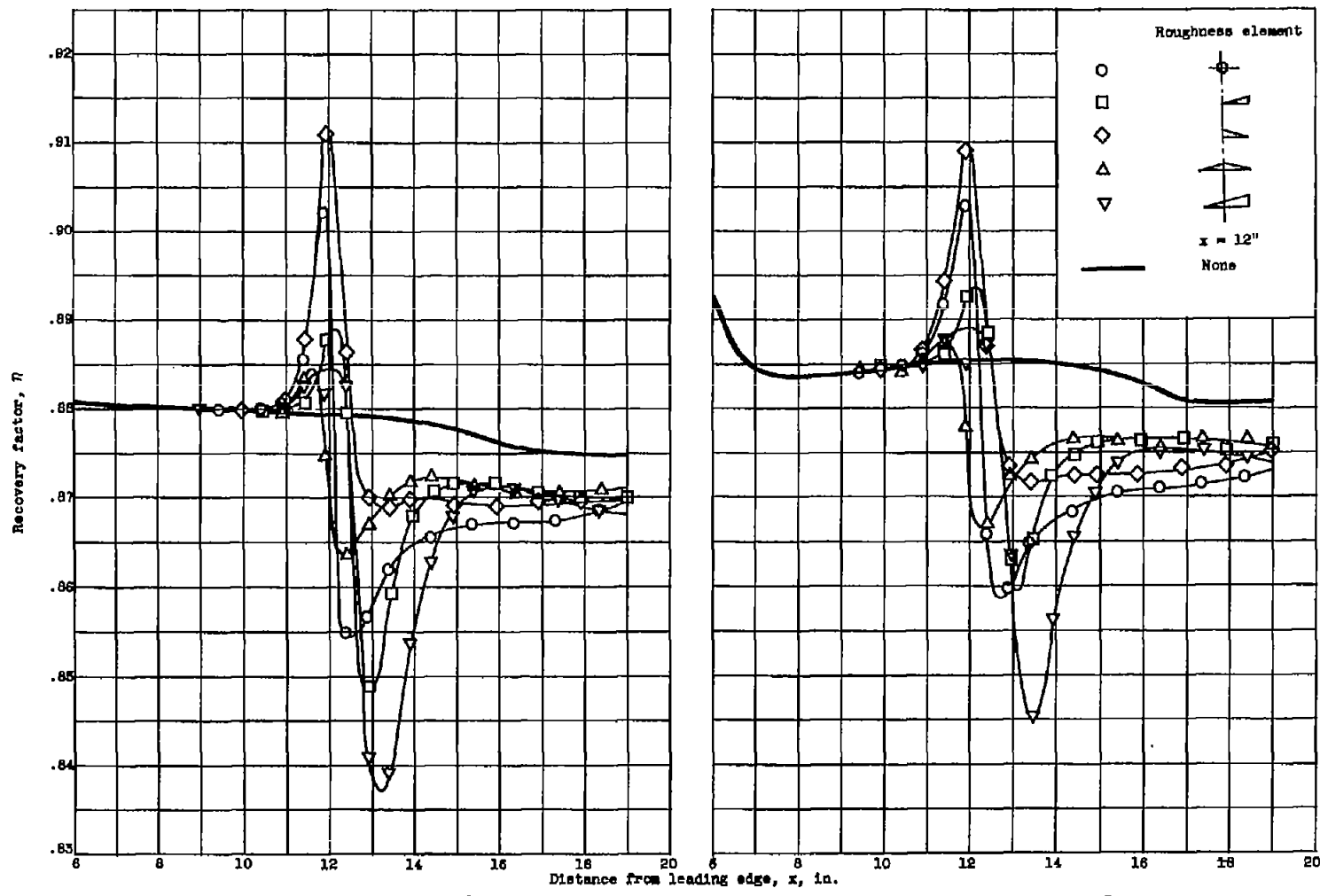
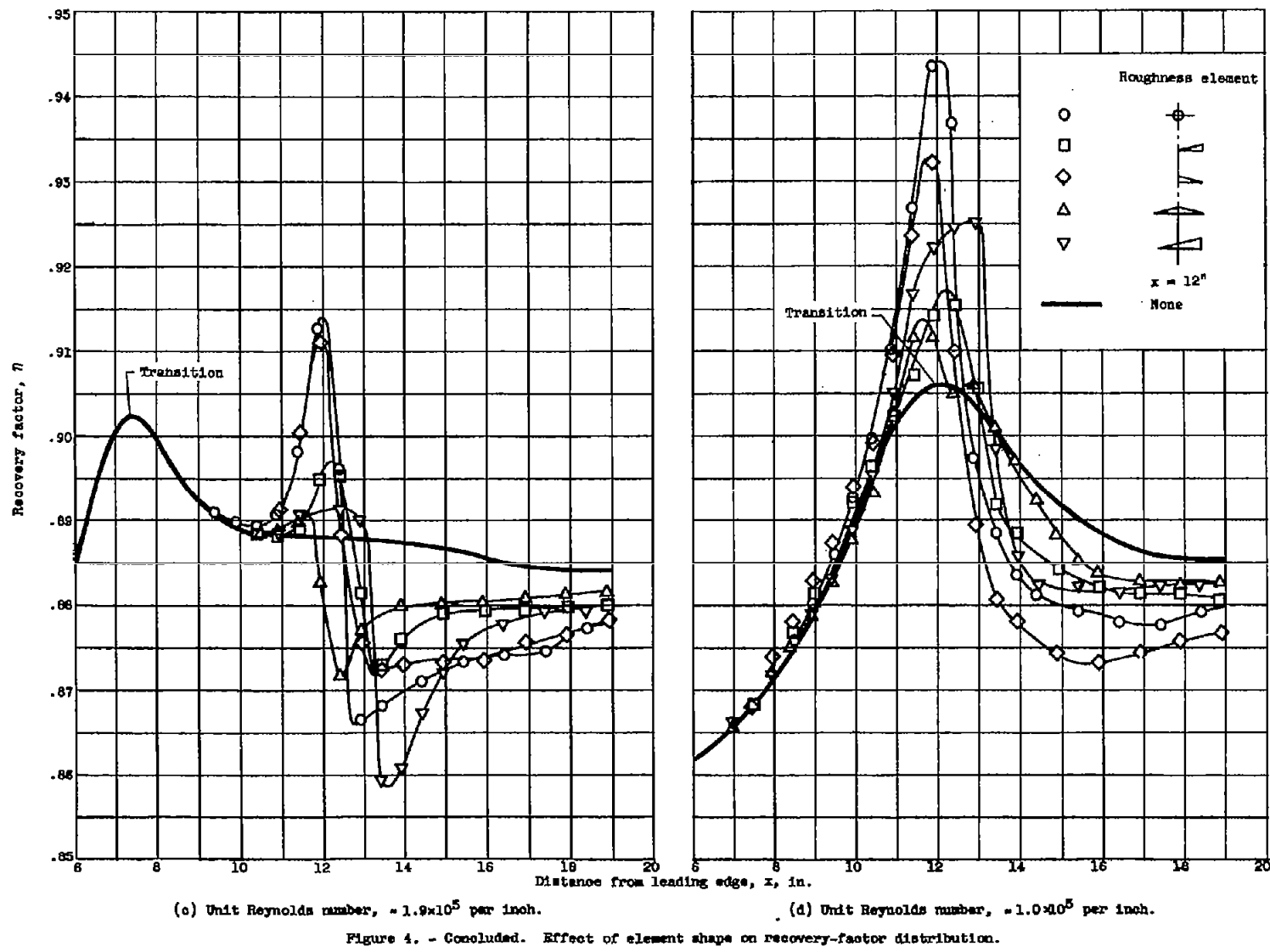


Figure 4. - Effect of element shape on recovery-factor distribution.



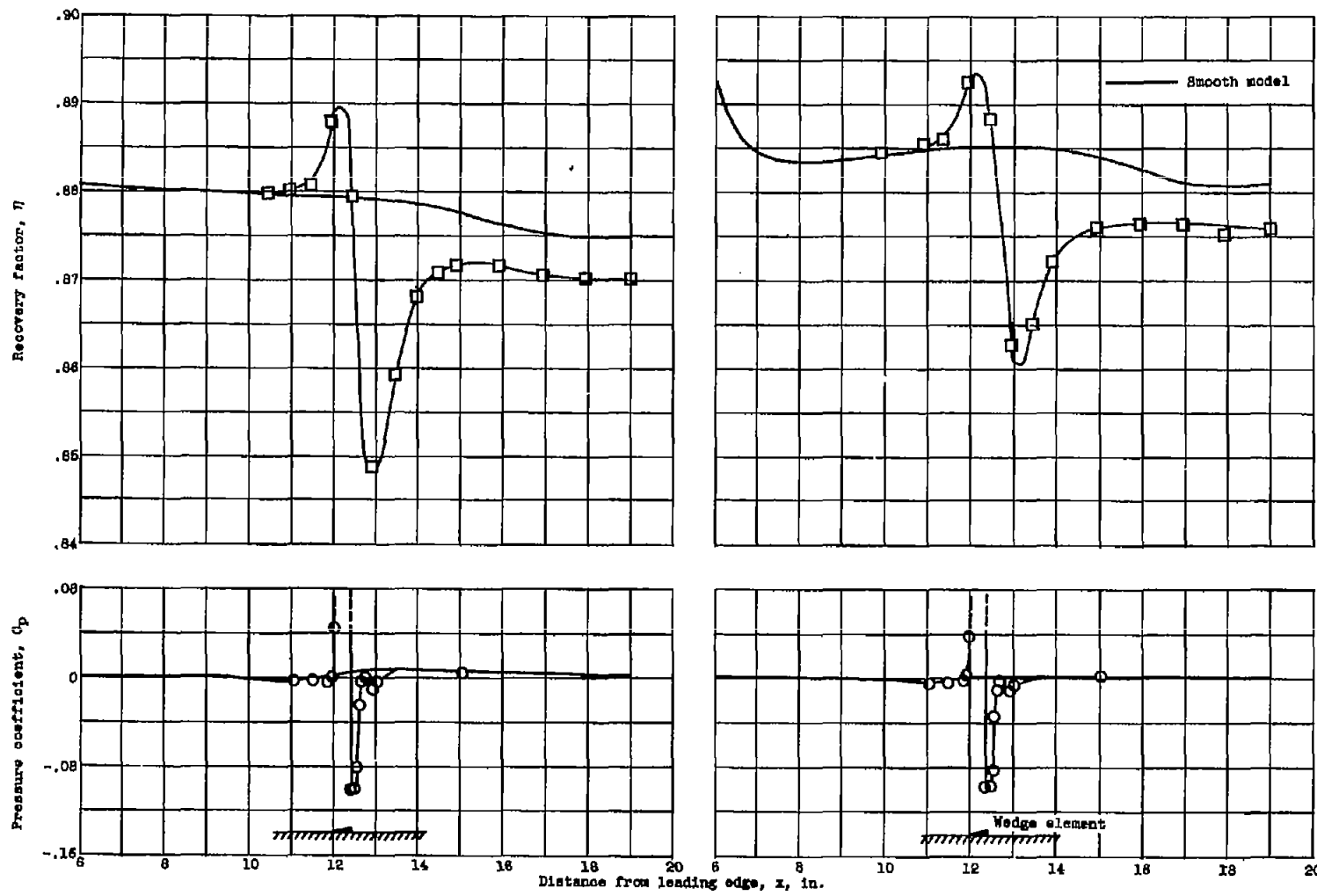
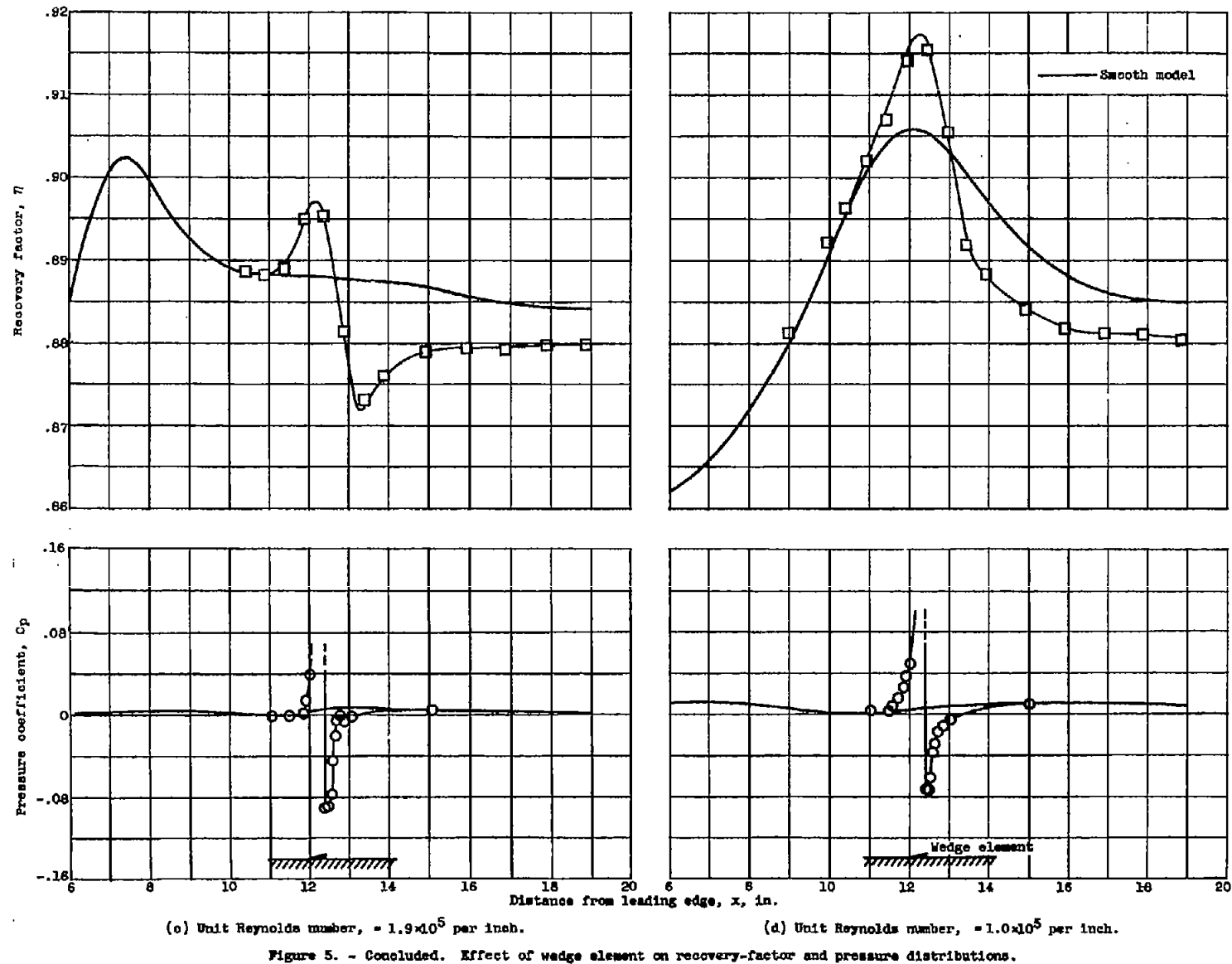


Figure 5. -- Effect of wedge element on recovery-factor and pressure distributions.



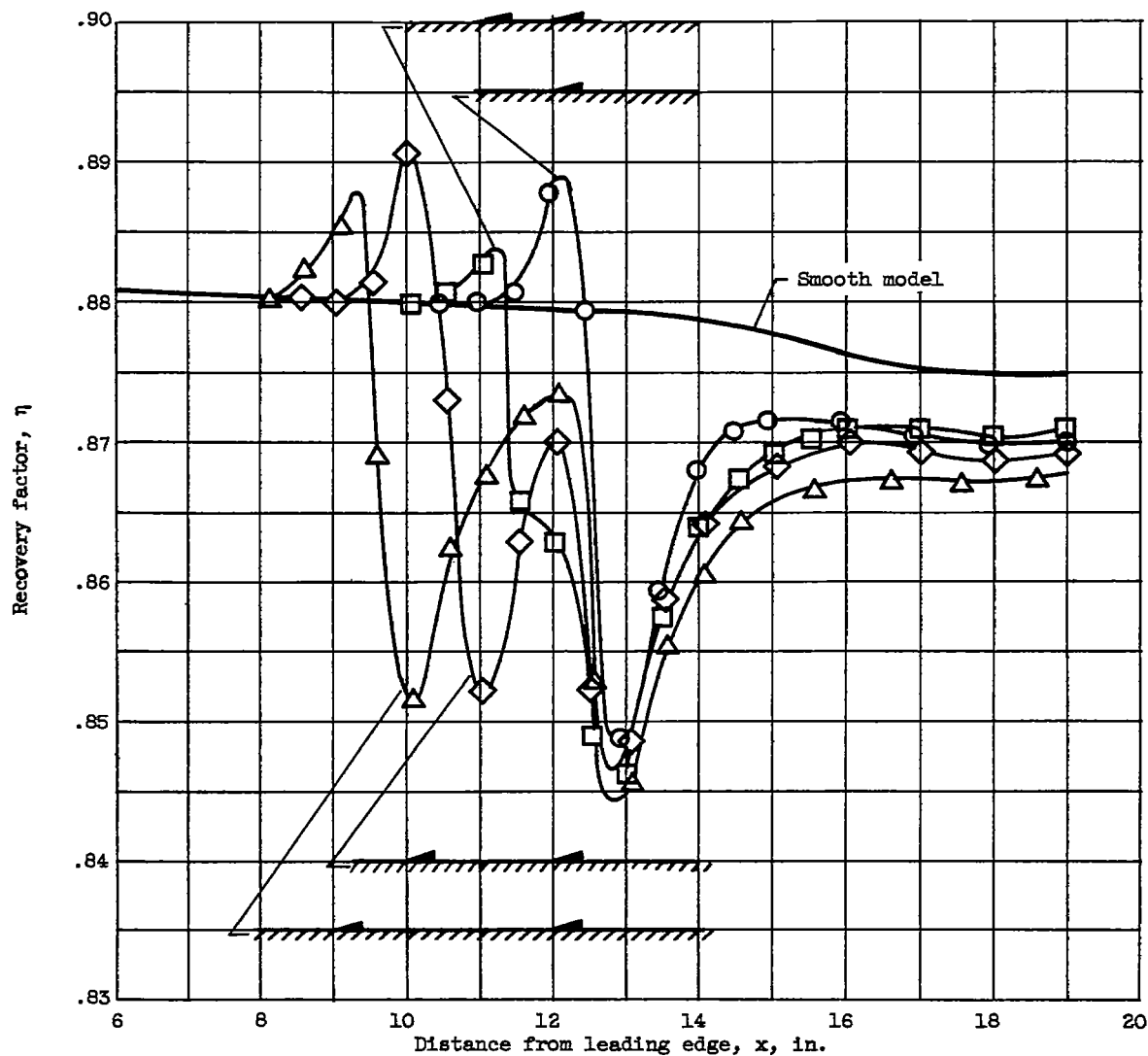


Figure 6. - Effect of wedge-element spacing on recovery-factor distribution. Unit Reynolds number,  $6.5 \times 10^5$  per inch.

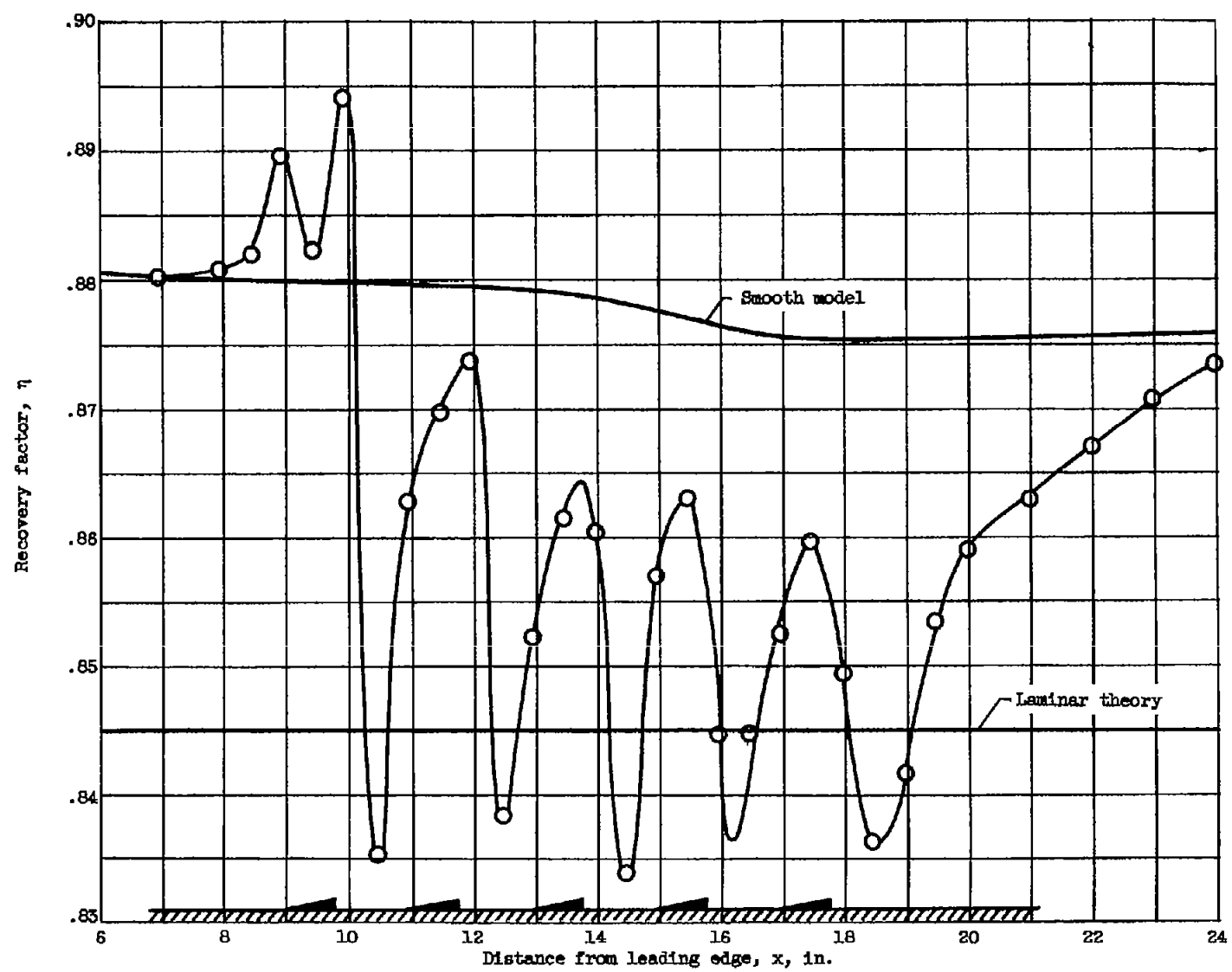


Figure 7. - Effect of multiple elements in turbulent boundary layer. Unit Reynolds number,  $6.5 \times 10^5$  per inch.

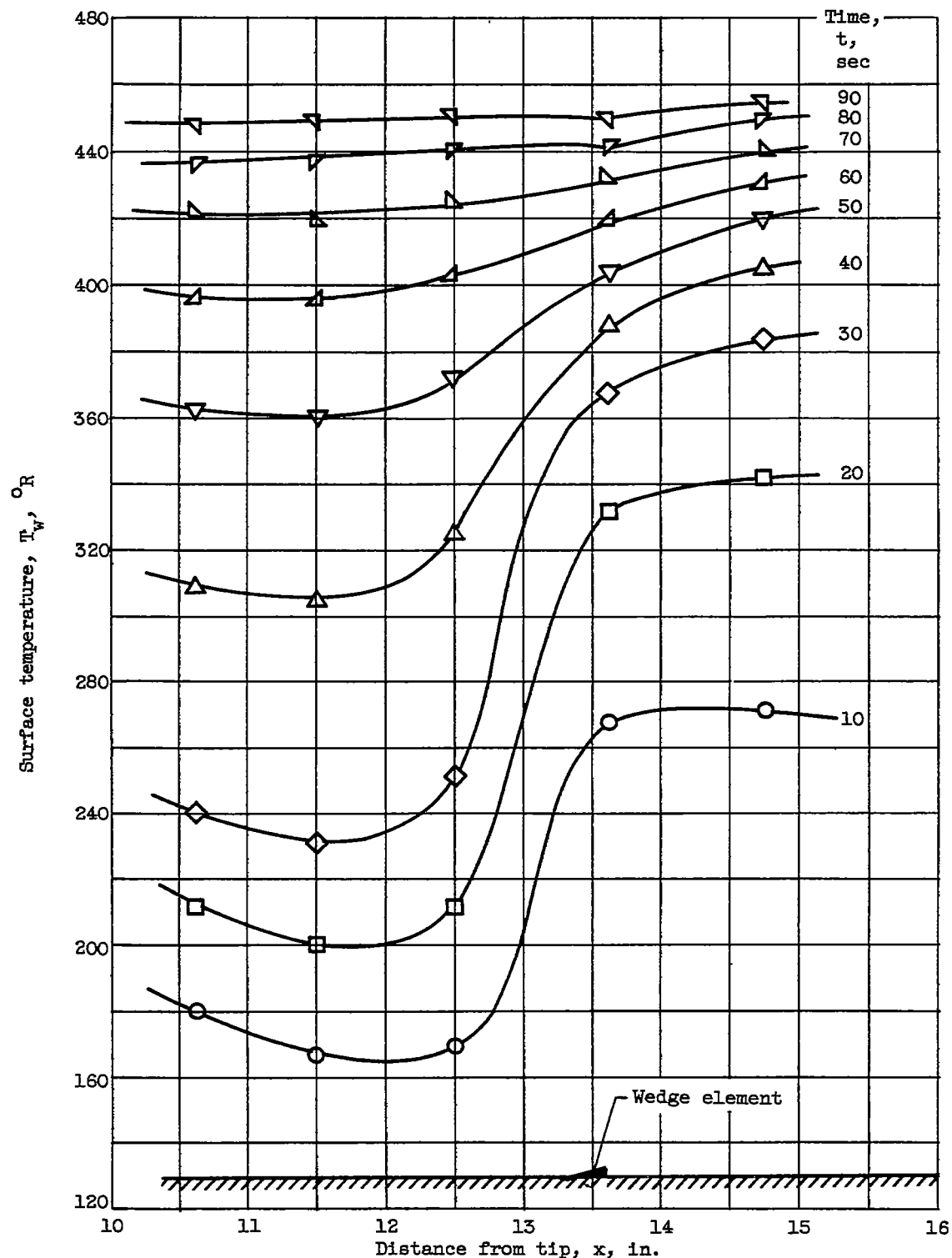


Figure 8. - Temperature distributions at various times on cone-cylinder model.

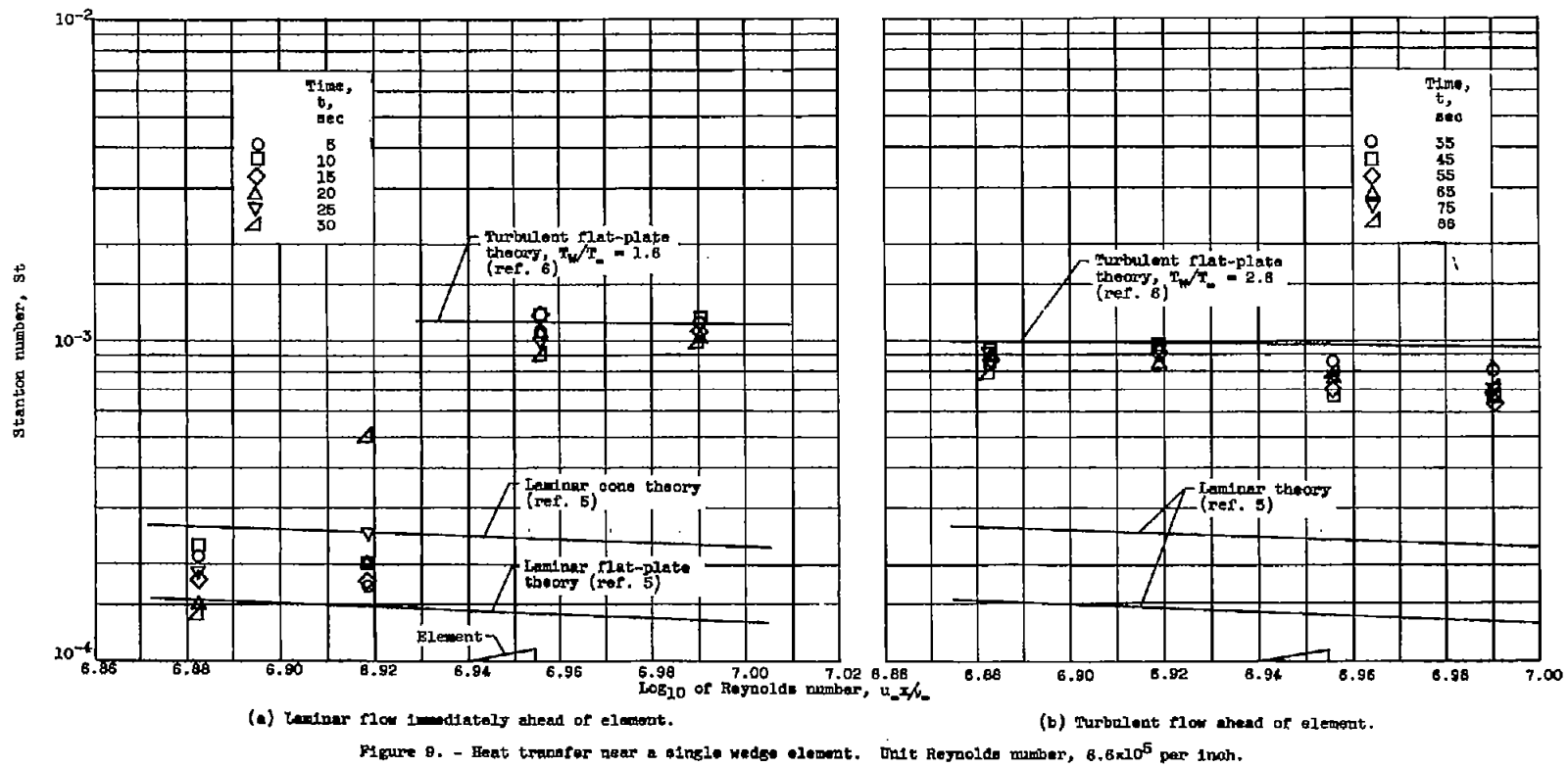


Figure 9. - Heat transfer near a single wedge element. Unit Reynolds number,  $6.8 \times 10^5$  per inch.